

there is no real contradiction between the two sets of deductions of deposition energies.

It has been mentioned earlier that the distributions of momentum, energy, and mass observed for fragments produced in bismuth fission are very much like those observed for the noncollinear events in uranium if a simple adjustment is made for the 14% mass increase. Specifically, there is no evidence for fission fragments having kinetic energies about $\frac{2}{3}$ the values observed radiochemically⁷ for neutron-excessive species, even though such low-energy neutron deficient species contribute substantially to the yield in a given mass region.² In fact, for bismuth the fragment velocity, averaged over all angles, which is obtained by appropriately weighting the velocities given in Table I, is 1.21

(MeV/amu)^{1/2}, the same, within the uncertainties, as the velocity from uranium fission at the same mean excitation energy 270 MeV.⁹ It may be concluded then that the bismuth fission mechanism is not distinguishable from that of uranium at high energies, and the latter as has already been shown does not differ from the mechanism of low-energy fission.

ACKNOWLEDGMENTS

The authors are indebted to Joseph Lypecky, John Hennessy, and Robert Stafford for assistance in setting up working arrangements at the Cosmotron and to J. W. Glenn, III and the Cosmotron operating staff. They wish to thank Evelyn Ritter for preparing the targets used in these experiments.

Production of the Light Elements Lithium, Beryllium, and Boron by Proton Spallation of ¹²C†

CARY N. DAVIDS,* HELMUT LAUMER, AND SAM M. AUSTIN

Cyclotron Laboratory, Physics Department, Michigan State University, East Lansing, Michigan 48823

(Received 30 July 1969)

Cross sections for the production of the light elements lithium, beryllium, and boron by proton bombardment of ¹²C were measured for proton energies between 21.7 and 44.0 MeV. Time-of-flight methods were used to identify the masses of ions recoiling from a thin target into a semiconductor detector. The results are related to current models on the origin of these light elements, and are consistent with a suggestion that the ¹¹B/¹⁰B isotopic ratio has remained unaltered at its formation value.

I. INTRODUCTION

THE origin of the light elements lithium, beryllium, and boron (LiBeB) is an interesting astrophysical problem. These elements are negligibly present in the sequence of charged-particle fusion reactions which synthesize heavier elements from hydrogen and helium. In addition, they are too fragile to survive the temperatures found in the deep interiors of stars, the site of nearly all the element-synthesizing nuclear processes. It was originally suggested by Fowler *et al.*¹ that the LiBeB isotopes were produced on the surfaces of stars by proton spallation of heavier elements.²⁻⁴ In later

articles,^{5,6} they expanded this suggestion, and incorporated it into a model for the origin of the planets. In their scheme the site of the spallation reactions was in meter-sized "icy planetesimals," remote from the early sun, but coupled to it by magnetic forces. Protons, originating from surface flares and having a mean energy of 500 MeV, would spiral along the magnetic lines of force and bombard the planetesimals. The LiBeB would be produced primarily from the targets ¹⁶O, ²⁴Mg, and ²⁸Si.

In the absence of cross-section data, the authors assumed that the production values of the isotopic ratios ⁷Li/⁶Li and ¹¹B/¹⁰B were unity. In addition to the LiBeB, large numbers of neutrons would be produced. After thermalization these neutrons would react with ⁶Li and ¹⁰B, which both have large low-energy neutron cross sections, thus depleting these isotopes and producing the observed terrestrial and meteoritic ⁷Li/⁶Li and ¹¹B/¹⁰B isotopic ratios of 12.5 and 4.1, respectively.⁷

With the development of mass spectrometric tech-

† Work supported in part by the National Science Foundation.

* Present address: Center for Nuclear Studies, University of Texas, Austin, Tex. 78712.

¹ W. A. Fowler, G. R. Burbidge, and E. M. Burbidge, *Astrophys. J. Suppl.* **2**, 167 (1955).

² Recent calculations of big-bang nucleosynthesis (Ref. 3) indicate the possibility of synthesizing ⁷Li in a cosmic fireball, but no ⁶Li or heavier elements are produced. Computations of nucleosynthesis in exploding objects (Ref. 4) yield ⁷Li, ⁹Be, ¹⁰B, and ¹¹B in addition to heavier elements, but again no observable ⁶Li is produced. These two cases do not diminish the importance of the spallation hypothesis, but do provide possible alternative routes for synthesizing *some* of the LiBeB.

³ R. V. Wagoner, W. A. Fowler, and F. Hoyle, *Astrophys. J.* **148**, 3 (1967).

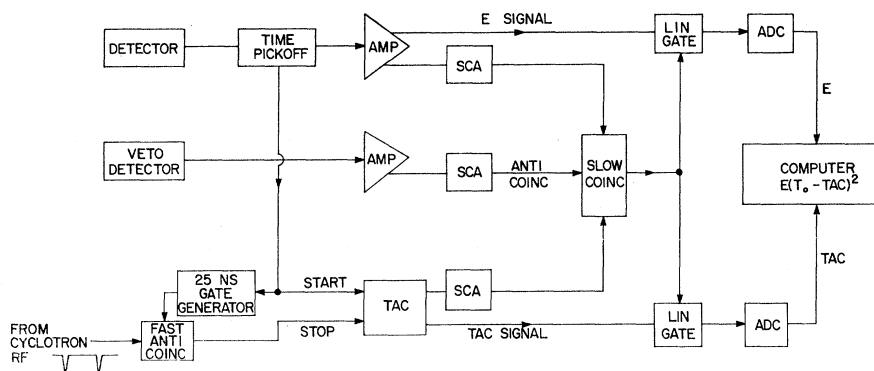
⁴ R. V. Wagoner, *Astrophys. J. Suppl.* **162**, 247 (1969).

⁵ W. A. Fowler, J. L. Greenstein, and F. Hoyle, *Geophys. J.* **6**, 148 (1962).

⁶ D. S. Burnett, W. A. Fowler, and F. Hoyle, *Geochim. Cosmochim. Acta* **29**, 1209 (1965).

⁷ M. Shima, *J. Geophys. Res.* **67**, 4251 (1962); D. Krankowsky and O. Muller, *Geochim. Cosmochim. Acta* **28**, 1625 (1964).

FIG. 1. Block diagram of charged-particle time-of-flight electronics.



niques enabling identification of extremely small quantities of LiBe isotopes,⁸ the Orsay mass spectrometry group was able to begin measuring spallation cross sections in ^{12}C and ^{16}O at several energies.^{9,10} On the basis of their experimental results and studies of the systematics of spallation reactions, they formulated a different theory of the origin of LiBeB.¹¹ They suggested that each star produces LiBeB in the stellar atmosphere by proton spallation of the abundant elements ^{12}C , ^{14}N , ^{16}O , and ^{20}Ne . In their scheme the solar system $^{11}\text{B}/^{10}\text{B}$ ratio remains unchanged from its formation value, but the $^7\text{Li}/^6\text{Li}$ ratio has increased from the production value of about 2.5 to its observed value of 12.5. This change is ascribed to (p, α) reactions on ^6Li at temperatures which would be found near the bottom of the convection region of the primitive sun. Under these conditions the isotopes ^7Li , ^9Be , ^{10}B , and ^{11}B are depleted only negligibly. Thus the need for neutrons to deplete ^6Li and ^{10}B is removed, and the site of the LiBeB

production is placed in the stellar atmosphere. The presence of icy planetesimals is not essential to their theory, thereby relaxing the requirement of high energy for the bombarding protons.

Experimental proton spallation cross sections for LiBeB are required to test the validity of the various approaches. In particular, knowledge of the $^{11}\text{B}/^{10}\text{B}$ formation ratio should enable one to choose between the speculations outlined above. The targets of interest are ^{12}C , ^{14}N , ^{16}O , ^{20}Ne , ^{24}Mg , and ^{28}Si , while proton energies from threshold to somewhat below 100 MeV are most important for the production of LiBeB. The observed steep energy behavior of the proton flux from solar flares ($\sim E^{-4}$) markedly reduces the contribution from protons with higher energies.

The available data on production cross sections have recently been reviewed.¹² Most of the cross sections have been measured by radioactivity and mass spectrometric techniques. Little information is available on the production of ^9Be , ^{10}B , and ^{11}B , particularly for energies below 100 MeV.

A program has been initiated in this laboratory to measure spallation cross sections relevant to the production of LiBeB. The $A = 10$ and $A = 11$ data have been reported in Ref. 13. Reported here are the results on production of isotopes with $6 \leq A \leq 11$ from a target of ^{12}C , for proton bombarding energies between 21.7 and 44.0 MeV.

II. EXPERIMENTAL METHOD

The techniques that have been used for measuring spallation cross sections, namely, radioactivity and mass spectrometry, each suffer from the disadvantage of not being equally sensitive to all isotopes simultaneously. The determination of a total production cross section by the usual methods of nuclear physics involves measuring the angular distribution of the reaction products and integrating this quantity over all angles. In order to apply this method to the present problem, it is neces-

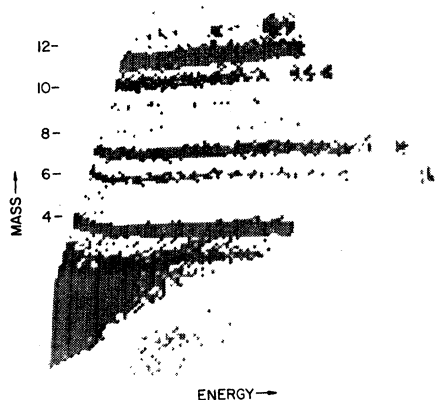


FIG. 2. Computer oscilloscope display of ET^2 (mass) versus E , showing mass bands.

⁸ E. Gradsztajn, M. Epherre, and R. Bernas, *Phys. Letters* **4**, 257 (1963).

⁹ R. Bernas, M. Epherre, E. Gradsztajn, R. Klapisch, and F. Yiou, *Phys. Letters* **15**, 147 (1965).

¹⁰ F. Yiou, M. Baril, J. DuFaure de Citres, P. Fontes, E. Gradsztajn, and R. Bernas, *Phys. Rev.* **166**, 968 (1968).

¹¹ R. Bernas, E. Gradsztajn, H. Reeves, and E. Schatzman, *Ann. Phys. (N.Y.)* **44**, 426 (1967).

¹² J. Audouze, M. Epherre, and H. Reeves, in *High-Energy Nuclear Reactions in Astrophysics*, edited by B. S. P. Sien (W. A. Benjamin, Inc., New York, 1967), p. 255.

¹³ C. N. Davids, H. Laumer, and S. M. Austin, *Phys. Rev. Letters* **22**, 1388 (1969).

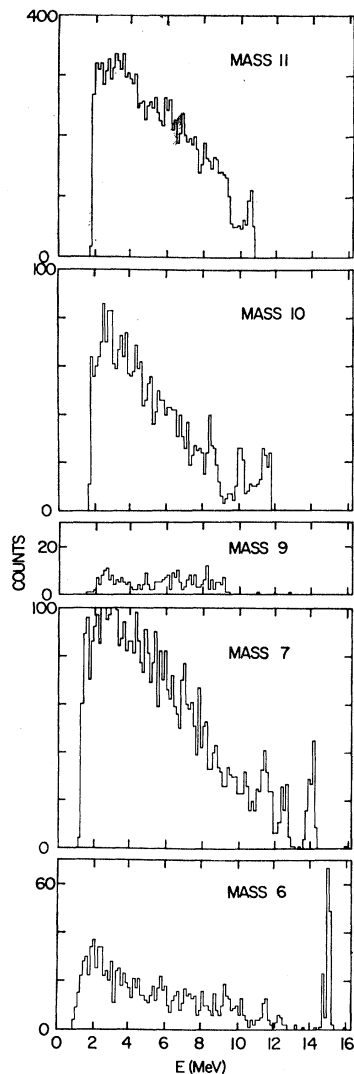


FIG. 3. Energy spectra of the various masses following the bombardment of ^{12}C by 39.8-MeV protons. The detector angle was 15° from the beam direction.

sary to ensure that (1) the target used is thin enough to allow the ions to emerge from it and proceed to the detector and (2) the detection system is able to identify and separate the isotopes of interest.

The first requirement is satisfied by a ^{12}C target with thickness less than about $100 \mu\text{g}/\text{cm}^2$; the maximum energy lost by a recoiling particle is then less than 0.65 MeV, this loss occurring for a 4.4-MeV ^{11}C ion.

Particle identification can be accomplished in several ways. Two semiconductor counters in series, acting as energy loss (ΔE) and stopping (E) detector, respectively, can separate the various ions by mass and charge. However, ions stopping in the front detector cannot be identified. Because a large number of the heavier fragments produced by spallation have low energy, this is a serious limitation.

A second method, which avoids this difficulty, is to measure the total energy (E) and the time-of-flight (T) of each ion as it stops in a single detector. Such a measurement gives the particle mass (M), through the relation $ET^2 = MD^2/2$, where D is the flight distance between target and detector. Knowing the mass turns out to be sufficient for the present purpose, as is explained in Sec. III below. Only the sensitivity of the time measurement circuit connected to the detector sets the lower energy limit. In addition, the system can be made insensitive to elastically scattered protons and other energetic light particles by proper choice of detector thickness.

A knowledge of the precise time that the ion left the target is required in order to apply this method. Such information is readily available using a pulsed beam, and the narrow ($\lesssim 0.2$ nsec) burst width of the proton beam from the MSU sector-focused cyclotron is eminently suited to such a precise timing application. For all these reasons, the ET^2 particle identification method was chosen for this experiment.

Thin self-supporting ^{12}C targets were made by dipping a glass slide into a colloidal graphite suspension, allowing it to dry, and floating off the resulting thin films on water. Typical targets had thicknesses between 65 and $80 \mu\text{g}/\text{cm}^2$, with less than 6% oxygen contamination. The target thickness was measured by comparing the elastic scattering yield from the unknown with the yield from a thick target. The thick target, in turn, was measured by an α -particle thickness gauge and also by weighing. An over-all uncertainty of $\pm 10\%$ due to the target thickness measurement has been assigned to the absolute cross sections.

A block diagram of the electronics is shown in Fig. 1.

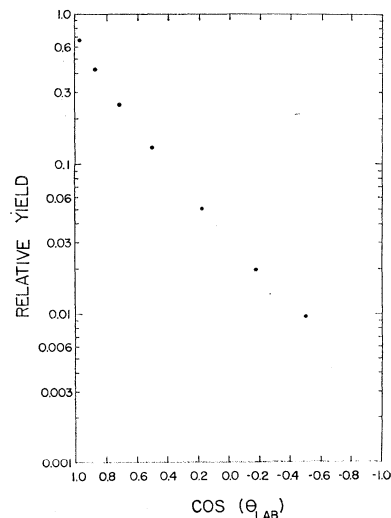


FIG. 4. Angular distribution of mass-7 particles measured at 39.8-MeV bombarding energy. The abscissa is $\cos\theta_{\text{lab}}$, so that the area under the curve is a measure of the total cross section. It is clear that the extrapolations to 0° and 180° introduce very little error.

A fast timing signal was derived from the fully depleted surface-barrier detector by means of an Ortec model 260 time pickoff. Cooling the detector with a dry ice and alcohol system resulted in improved time response. The dead layer of the detector caused energy losses for the heaviest ions which did not exceed 0.1 MeV. Detectors of thickness 78 and 68 μm were used, depending on the proton bombarding energy, with flight distances of the order of 28 cm. The time-to-amplitude converter (TAC) was started by a signal from the detector, and stopped by the next rf pulse from the cyclotron. This caused the time spectrum to be inverted, i.e., to be proportional to the quantity $T_0 - T$, where T_0 is a constant, but ensured that the TAC was busy only for a real event. In addition, a fixed time of approximately 25 nsec was electronically added to each time interval measured, so that only the linear portion of the TAC was utilized. Maximum flight times between 52 and 72 nsec were determined by the cyclotron rf period at the various bombarding energies. This imposed a lower limit on the observable energies for the heavier masses, which fell between 1 and 2 MeV for the $A = 11$ ions. The lower limit for ^6Li was set by the sensitivity of the time pickoff, and was typically 0.8 MeV. The veto counter caused the rejection of any particle which passed through the front detector.

The two signals E and TAC were digitized and sent to the Sigma-7 computer. Here, by means of the general-purpose code ROOTSIE,¹⁴ the quantity $E(T_0 - \text{TAC})^2$ was computed on line. This quantity is proportional to ET^2 for the correct value of T_0 and, when displayed

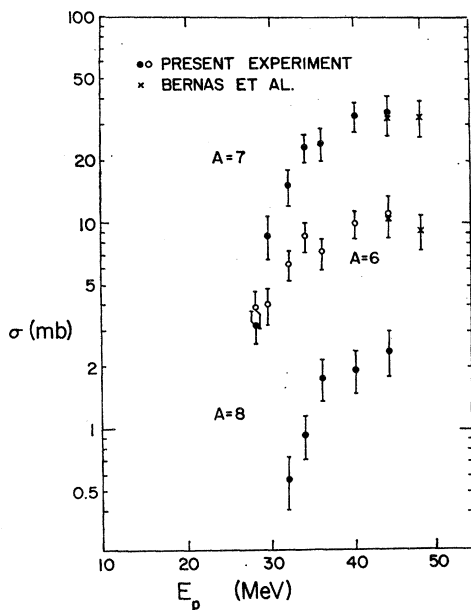


FIG. 5. Production cross sections of masses 6-8 from proton spallation of ^{12}C . The error bars represent the total uncertainty.

¹⁴ D. Bayer (private communication).

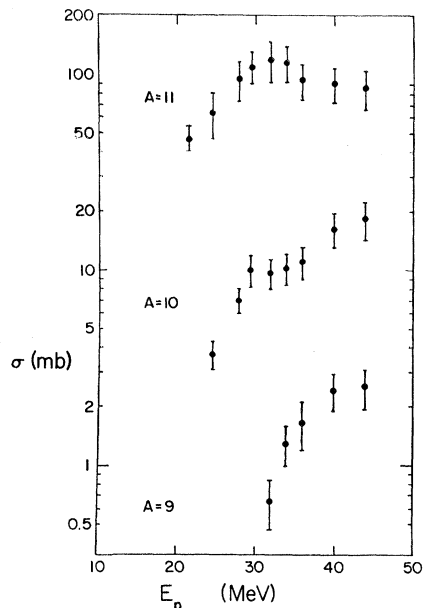


FIG. 6. Production cross sections of masses 9-11 from proton spallation of ^{12}C . The error bars represent the total uncertainty.

versus E , causes the different masses to fall in bands. The parameter T_0 is adjusted by teletype input until the bands appear approximately horizontal on the display. A typical display of ET^2 versus E is shown in Fig. 2. The size of this array is 128×128 channels.

Using such a two-dimensional display, a given mass band can be outlined by computer-generated curves placed between the bands, and the events lying between two curves are projected on the E axis. In this way, energy spectra for all the masses of interest can be obtained. Figure 3 shows spectra taken at a proton energy of 39.8 MeV, with the detector at an angle of 15° to the beam.

The peaks appearing in some of the spectra are due to reactions involving only two bodies in the final state, with the possibility that the detected particle and also the residual nucleus can be left with excitation. Only particle-stable states of the ion of interest will be observed, and all γ decays occur before the particle reaches the detector. These two-body reactions only account for a small percentage of the total yield for each isobar.

In general, the reactions proceed through multibody channels; the continuum in the energy spectrum is caused by the superposition of yields from multibody final states of differing total energies, e.g., the mass-11 yield is due to the reactions $^{12}\text{C}(p, d)^{11}\text{C}$, $^{12}\text{C}(p, pn)^{11}\text{C}$, and $^{12}\text{C}(p, 2p)^{11}\text{B}$, where in each case the ^{11}C and ^{11}B ions can be left in the ground state or in any of their particle-stable excited states. For the latter two reactions this means that the three-body system can emerge with eight or nine values of total kinetic energy. The sum of the many three-body distributions causes the spectrum to be peaked at low energy, but it must

TABLE I. Production cross sections from proton spallation of ^{12}C .

E_p (MeV)	$\sigma(6)$ (mb)	$\sigma(7)$ (mb)	$\sigma(8)$ (mb)	$\sigma(9)$ (mb)	$\sigma(10)$ (mb)	$\sigma(11)$ (mb)
21.7	45±7
24.6	3.7±0.6	64±17
28.0	3.9±0.8	3.2±0.6	7.0±1.1	96±22
29.5	4.0±0.8	8.7±2.1	10.0±1.8	113±20
32.0	6.3±1.0	15.2±3.0	0.6±0.2	0.7±0.2	9.7±1.7	121±28
34.0	8.6±1.4	23.2±3.7	0.9±0.2	1.3±0.3	10.2±1.8	116±25
36.0	7.2±1.1	24.1±4.2	1.8±0.4	1.7±0.4	11.1±2.1	95±21
39.8	9.9±1.5	33.1±5.4	1.9±0.5	2.4±0.5	16.3±3.3	91±18
44.0	11.2±2.2	34.4±6.6	2.4±0.6	2.5±0.6	18.4±4.1	87±20

have the value zero at zero energy. This is because the Jacobian of the transformation from c.m. to laboratory coordinates is equal to the ratio p/\bar{p} , where p and \bar{p} are the momenta in the laboratory and c.m. systems, respectively. In the spectra of Fig. 3, the peaking at low energies and down-turn toward zero at zero energy are evident for all masses except for mass 9. This unique case ^9Be is probably produced via the reaction $^{12}\text{C}(p, p^3\text{He})^9\text{Be}$, which has only one open three-body channel. Thus no low-energy peak is expected.

Spectra were accumulated at seven or eight angles, ranging between 15° and 120° for the higher bombarding energies, and to smaller back angles for lower-energy runs. Angular distributions were measured at proton bombarding energies of 44.0, 39.8, 36.0, 34.0, 32.0, 29.6, 28.0, 24.6, and 21.7 MeV, as determined by the beam transport system analyzing magnets. For each run the product of target thickness and incident charge was normalized by means of a fixed monitor counter, which measured the protons elastically scattered from ^{12}C .

The individual energy spectra at each angle were extrapolated to zero energy in order to obtain the total yield. Allowance for the missing portions has been made by adding to the observed totals a representative average number of counts per channel for the energies below the low-energy cutoff. At each angle, half of the resulting contribution to the total cross section has been assigned as a conservative uncertainty. Added together, these errors account for most of the 15–30% uncertainty quoted for the final absolute cross sections. In all cases, the yields decreased rapidly as the detector was moved to back angles. Figure 4 shows a typical angular distribution, in this case measured for the mass-7 particles at 39.8 MeV. Extrapolation of the angular distributions to 0° and 180° produced an additional small uncertainty in the final result.

The experimental angular distributions were converted to absolute cross sections using the known solid angle, target thickness, and charge accumulation. A Faraday cup was used to provide the relation between incident charge and elastic yield as determined by the monitor counter.

III. RESULTS AND DISCUSSION

The total cross sections obtained from these measurements are given in Table I, and shown in Figs. 5 and 6, plotted against proton bombarding energy. Included are the mass spectrometry measurements of Bernas *et al.*⁹ on mass-6 and mass-7 production in this energy region. Our results show good agreement with the mass spectrometry results where the two overlap.

For our proton bombarding energies, the mass-6 particles are ^6He and ^6Li . The mass-7 particles are ^7Li and ^7Be , while ^8B and ^9Be make up masses 8 and 9, respectively. Mass 10 consists of ^{10}Be , ^{10}B , and ^{10}C , with ^{11}B and ^{11}C comprising the mass-11 yield. It should be noticed that there is only one stable isobar for each mass (except for mass 8, which has none), and the radioactive isobars decay rapidly to it on an astrophysical time scale.¹⁵ Thus for our purposes, a mass measurement is sufficient, and (mass 6) $\equiv ^6\text{Li}$, (mass 7) $\equiv ^7\text{Li}$, (mass 9) $\equiv ^9\text{Be}$, (mass 10) $\equiv ^{10}\text{B}$, and (mass 11) $\equiv ^{11}\text{B}$.

A calculation of the abundances and isotopic ratios of the LiBeB elements produced by spallation could in principle be carried out. What is required are the experimental production cross sections as a function of energy, the abundances of the targets involved, and knowledge of the proton spectrum at the stellar surface. The results of such a calculation, when compared with the observations, would serve as a basis for determining whether or not other nuclear processes have been involved in the history of these elements. Fractionation, weathering, and other chemical effects must also be considered.

On the other hand, the isotopic ratios by themselves serve to provide information on the unique nuclear history of the LiBeB elements, since these ratios are unaffected by chemical processes.

From Fig. 5, it is seen that the production of ^{11}B from ^{12}C far exceeds that of ^{10}B . Using these cross sections and a proton spectrum varying as E^{-4} , a calculated $^{11}\text{B}/^{10}\text{B}$ ratio of about 8 is obtained for ^{12}C .

¹⁵ Although ^{10}Be could be considered stable with its half-life of 2.7×10^6 yr, its production rate is expected to be negligible compared with the total mass-10 yield (Refs. 10, 11).

For the over-all $^{11}\text{B}/^{10}\text{B}$ ratio, one must consider the production of ^{11}B and ^{10}B separately from all the targets, weighted by the appropriate abundances. The solar photospheric abundances of the important targets ^{12}C , ^{14}N , and ^{16}O are in the approximate ratios 3:1:5.¹⁶ Because of differing values of production thresholds, each of these three targets might be expected to contribute about equally to the formation of ^{11}B and ^{10}B . Preliminary values obtained in this laboratory for the $^{11}\text{B}/^{10}\text{B}$ ratios at 35 MeV for ^{14}N and ^{16}O are 0.5 and 8, respectively. Below 12 MeV only ^{11}B is produced from ^{14}N , via the $^{14}\text{N}(p, \alpha)^{11}\text{C}$ reaction. These results are consistent with the suggestion of Barnas *et al.*¹¹ that the solar system $^{11}\text{B}/^{10}\text{B}$ formation ratio has not been altered by subsequent nuclear processes.

The low value of the ^9Be production cross section is not surprising, in view of the fact that this nucleus has only one particle-stable state, compared to the nine or so states available in ^{11}B and ^{11}C . In addition, the

¹⁶ E. A. Muller, in *Origin and Distribution of the Elements*, edited by L. H. Ahrens (Pergamon Press, Oxford, 1968), p. 155.

formation of ^9Be via the direct $(p, p^9\text{He})$ reaction is expected to depend strongly on the probability of finding ^3He clusters in the target nucleus, a situation likely to occur only infrequently.

Production of ^7Li from ^{12}C exceeds that of ^6Li by a factor of 2-3, in agreement with the estimates of Barnas *et al.*¹¹ A large $^7\text{Li}/^6\text{Li}$ ratio near threshold was not observed. Such a large ratio might have made it possible to explain the terrestrial and meteoritic $^7\text{Li}/^6\text{Li}$ ratio if, in addition, a spectrum of protons with energies extending only to about 25 MeV were postulated. The necessity of a secondary process to explain the terrestrial $^7\text{Li}/^6\text{Li}$ ratio remains, the most likely candidate being the $^6\text{Li}(p, \alpha)$ reaction. Slow neutrons do not seem to be the answer, since they would increase the $^{11}\text{B}/^{10}\text{B}$ ratio further.

Further measurements of proton spallation cross sections for LiBeB production from ^{14}N , ^{16}O , and heavier targets, as well as additional measurements on ^{12}C at higher energies, are required. It is hoped that such results will soon be available, enabling a better understanding of the origin of lithium, beryllium, and boron.

(d, p) and (d, t) Reaction Studies of the Actinide Elements. I. U^{235} †

T. H. BRAID, R. R. CHASMAN, J. R. ERSKINE, AND A. M. FRIEDMAN

Argonne National Laboratory, Argonne, Illinois 60439

(Received 2 September 1969)

Levels of the nucleus U^{235} , populated in the reactions $\text{U}^{234}(d, p)\text{U}^{235}$ and $\text{U}^{236}(d, t)\text{U}^{235}$ induced by 12-MeV deuterons from the Argonne tandem Van de Graaff, were analyzed with a magnetic spectrograph. Most of the observed levels were identified as members of rotational bands built on the single-particle states of a deformed central field. The level assignments were made on the basis of relative populations of presumed members of each rotational band, ratios of the cross sections at 90° and 140° , and $(d, p)/(d, t)$ cross-section ratios. Pairing effects were calculated for the observed spectrum, and a single-particle scheme was extracted from the data. This single-particle scheme was compared with the calculations of Nilsson and Rost. Levels not predicted on the basis of the single-particle models were observed at excitations as low as 700 keV. Some of these levels, presumably vibrational excitations, were found to have cross sections comparable to those of single-particle states.

I. INTRODUCTION

IN this paper, we report the results of an investigation of (d, p) and (d, t) reactions populating levels in U^{235} . The considerations that govern these single-neutron transfer reactions are quite different from those applicable to decay processes, and accordingly these studies have furnished a large amount of new information on levels in U^{235} . The differential cross sections measured for these reactions give detailed information which is not readily obtained in other ways. Our measurements, in conjunction with results obtained from

α -decay¹⁻³ and Coulomb-excitation^{4,5} studies of U^{235} , give a rather extensive picture of the low-energy excitations in this nucleus. We shall examine this picture in the present paper. In future papers, we shall utilize our (d, p) and (d, t) data to analyze levels in the

¹ S. A. Baranov, V. M. Koulakov, and S. N. Belenki, *Nucl. Phys.* **41**, 95 (1963).

² Irshad Ahmad, Ph.D. thesis, University of California Lawrence Radiation Laboratory Report No. UCRL-16888, 1966 (unpublished).

³ J. E. Cline, *Nucl. Phys.* **A106**, 481 (1968).

⁴ J. O. Newton, *Nucl. Phys.* **3**, 345 (1957).

⁵ F. S. Stephens, M. D. Holtz, R. M. Diamond, and J. O. Newton, University of California Lawrence Radiation Laboratory Report No. UCRL-17976, 1968 (unpublished); *Nucl. Phys.* **A115**, 129 (1968).

† Work performed under the auspices of the U.S. Atomic Energy Commission.

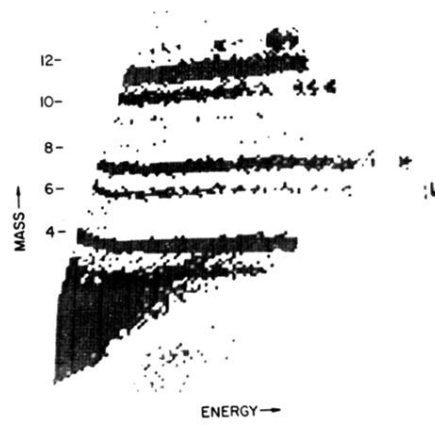


FIG. 2. Computer oscilloscope display of ET^2 (mass) versus E , showing mass bands.